

# Visco-hypoelastic model of photo-polymerization process for small changes of temperature

W. GAMBIN

*Faculty of Mechatronics  
Institute of Micromechanics and Photonics, Applied Mechanics Division  
Warsaw University of Technology  
Św. Andrzeja Boboli 8  
02-525 Warszawa, Poland  
e-mail: wgambin@mchtr.pw.edu.pl*

THE AIM OF THE PAPER is to propose a model for estimation of the shrinkage stress in photo-cured dental restorations. Up to now, the elastic and viscoelastic models of photo-curing process use an incremental approach with a large number of time steps, with a fixed Young's modulus and viscosity within each of the time increments. The elastic approach with a stepped increasing Young's modulus gives the stress values too high. On the other hand, the incremental viscoelastic approach requires long-lasting computations. In the present paper, a consistent model of the photo-curing process for the case of small temperature changes is proposed. The proposition bases on the Maxwell model, in which the Young's modulus and the viscosity are continuous functions of time. The assumptions of the model follow from the dental practice, as well as from a physical nature of the process and from the rules of continuum mechanics. A performed incremental analysis of the process enables to formulate an integral model of the process, with an explicit rule for the shrinkage stress for 1D and 3D cases. The model has been tested for the material data of dental composite Clearfil F2. Results of the calculations coincide with the values of stresses measured in thin layers of Clearfil F2.

**Key words:** photo-polymerization, shrinkage stress, dental composites, viscoelasticity, hypoelasticity, Maxwell model, time-dependent parameters.

Copyright © 2010 by IPPT PAN

## 1. Introduction

THE MOST POPULAR TECHNIQUE of tooth restoration is filling the tooth cavity with a photo-cured dental resin composite. However, after the curing process, a shrinkage stress appears in the dental filling. Shrinkage stresses generated in the composite during the process may result in a microleakage, which leads to a tooth decay. There are two ways of dealing with the problem of a shrinkage stress reduction. The first way is to select proper dental composites by testing of the chemical structure of cured materials [1–3]. The second way is to work out dental techniques reducing the shrinkage stresses [4–7]. In the last case,

the crucial point is the knowledge on the viscoelastic properties of the cured composites [8]. For each stage of the curing process, material parameters should be taken from adequate tests [1]. Then, on the basis of experimental data, one can model the cured material behavior in order to control the cure process and to reduce the shrinkage stresses. It is necessary to point out that during the considered process, one can observe small changes of temperature only. Then, one can assume that the thermal strains do not appear in the cured material. Because our goal is to propose a possibly simple model of the process with a clear physical interpretation of its behaviour, we neglect also the plastic effects. Taking the above into account, one can find in the literature two ways of the process modelling. According to the first way, we may neglect the viscous effects and use the elastic model with time-dependent elastic modules [4, 9]. In this case, to get the shrinkage stresses, one can use the standard numerical procedures for the hypoelastic materials [10–12]. If we want to involve the viscous effects, we may use an incremental procedure proposed in [13]. In this approach, the curing time is subdivided into a large number of small intervals, and Young's modulus as well as viscosity and current polymerization shrinkage are determined for each interval [14]. However, to determine the initial stresses at each time-step, it is necessary to perform extensive computations or to get the stress values from additional experiments [8]. Despite its drawbacks, the incremental approach is very popular. It enables to superpose, in incremental way, the elastic, the viscous, the thermal, and the plastic effects in one process<sup>1</sup>. Because the material behaviour is “frozen” during each of the small time-steps, one can introduce the models with a higher number of parameters. Nevertheless, a description of the global interactions between courses of various mechanical effects, during the whole process, is still an open question.

Below, an integral model of the photo-curing process with an explicit form of the shrinkage stress tensor is proposed. In the model, an influence of temperature changes on the shrinkage stress is neglected. It is due to the fact that during the dental restoration forming, we have to do with a relatively long time of irradiation with a low intensity [15]. It is not the case of the rapid-prototyping process, when we use a fast irradiation with high intensity [16]. The rate and the intensity of the irradiation determine a shrinkage rate during the whole process. In the proposed model, a current value of the shrinkage is taken as a measure of a polymerization degree [17]. Then, the value of the shrinkage stress depends directly on the shrinkage rate. Let us assume that the shrinkage rate is the sum of temporary elastic and viscous strain rates. The simplest rule which describes the elastic effects in the cured material is the hypoelastic one with a time-dependent

---

<sup>1</sup>Such an approach, known as the Dynamic Finite Element Method, is used in the numerical analysis of the stereolithography process [19–21].

Young's modulus. The viscous effects may be described by the linear viscous law with a time-dependent viscosity. Because the stress relaxation determines the final stress level, a choice of the Maxwell model with time-dependent parameters seems to be the most appropriate. Values of the Young modulus and the viscosity may be taken from the necessary material tests.

An analysis of the cured material behavior indicates that the shrinkage stress appears when the gel point is reached [14]. It means that two-thirds of the total shrinkage generates any stress, and the analysis of the process may be limited to its final phase. The incremental analysis of this stage is presented in Chapter 3. It shows interactions between the short-term elastic effects with the long-term viscous ones. The drawn conclusions lead to a formulation of 1D and 3D integral models of the cure process. Experimental data show that the Poisson coefficient decreases before the gel point; later one can assume it as a constant [14]. The assumption of a constant Poisson's coefficient put some restrictions on the relaxation of the Kirchhoff and the bulk modules in a 3D case (see Appendix). Calculations for the composite Clearfil F2 [1] show that the shrinkage stress in the cured material reaches the value 21 MPa. The obtained theoretical results coincide with the values of the shrinkage stresses measured in 100  $\mu\text{m}$ , thin composite layers [18]. The computations based on the hypoelastic model give the highest stresses nearly 70% larger. For a relaxed hypoelastic model, with an average relaxation time, we get the highest stress almost 30% lower.

## 2. Assumptions

The proposed model bases on three types of assumptions: those, which yield from the dental practice, those suggested by the physical nature of the cure process, and those coming from the rules of continuum mechanics.

### 2.1. Assumptions yielding from the dental practice

1. Photo-cured material for a dental restoration is a composite on the basis of a polymer or copolymer with a glass, ceramic or silanes as fillers.
2. Irradiation  $H$  [ $\text{mW}/\text{cm}^2$ ] takes place in the time  $t_0 \leq t \leq t_n$ . Usually,  $t_n - t_0$  equals 40~60 s.
3. An irradiation function  $H = H(t)$  takes values from the interval  $H_0 \leq H \leq H_{\max}$ , where  $H_0 = H(t_0)$  and  $H_{\max} = H(t_n)$ . In the dental practice, it is assumed that  $H = \text{const}$  (300~600  $\text{mW}/\text{cm}^2$ ).
4. An evolution of each of the mechanical properties is a function of light exposure  $E$  [ $\text{mJ}/\text{cm}^2$ ]. The quantity  $E = E(t)$  is connected with the irra-

diation function  $H = H(\tau)$  (for  $t_0 \leq \tau \leq t$ ) by the rule [16]:

$$(2.1) \quad E(t) = \int_{t_0}^t H(\tau) d\tau.$$

- Influence of the temperature change may be neglected because the temperature under a dental lamp fluctuates within the range  $\pm 5^\circ\text{C}$  [15]. It is due to a relatively long irradiation time (40 s) with low intensity. The above assumption is not valid in the case of the process of stereolithography, where a laser beam is used. There, the characteristic exposure time varies from 70  $\mu\text{s}$  to 2 ms [16].

## 2.2. Assumptions yielding from the physical nature of the process

- The cure process starts when the light exposure  $E$  attains a certain critical value  $E_c$ , at the time  $t_c > t_0$ . The ratio  $E_{\max}/E_c$  takes values 100~200 [16].
- As a measure of the polymerization degree (the degree of the monomer conversion), the volumetric shrinkage of the cured resin is taken [17]. The linear shrinkage is denoted by  $s$ , where  $0 \leq s \leq s_{\max}$ . Usually  $s \leq 1\%$ . The linear shrinkage is a function of the light exposure only,  $s = s(E(t))$ .

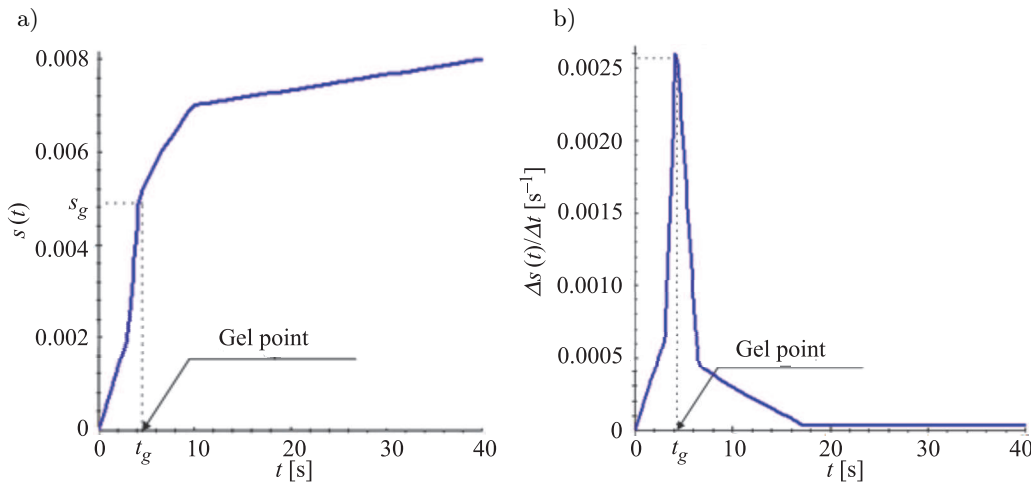


FIG. 1. Location of the gel point (according to experimental data given in [1]): a) on the shrinkage-time plot, b) on the shrinkage rate-time plot.

- The following mechanical properties of the cured composite have an influence on development of the shrinkage stress at the time  $t_c \leq \tau \leq t$ :
  - the Young modulus  $0 \leq Y(t) \equiv \bar{Y}(E(t)) \leq Y_{\max}$  (usually:  $Y_{\max} \sim 10$  GPa, for comparison:  $Y_{\text{enamel}} = 50$  GPa,  $Y_{\text{dentin}} = 12$  GPa [4]);

- the Poisson coefficient  $\nu_s \leq \nu(t) \equiv \bar{\nu}(E(t)) \leq \nu_r$ , where  $\nu_s$  is the coefficient of solid cured polymer, and  $\nu_r$  is Poisson's coefficient of the resin (usually:  $0.24 \sim 0.25 \leq \nu(E) \leq 0.48 \sim 0.5$ , for comparison:  $\nu_{\text{enamel}} = 0.3$ ,  $\nu_{\text{dentin}} = 0.23$  [4]);
  - viscosity  $0 \leq \eta(t) \equiv \bar{\eta}(E(t)) \leq \eta_{\text{max}}$  (usually  $\eta_{\text{max}} \approx 1000$  GPa · s).
4. The shrinkage stresses appear when the process attains the gel point – the stage at which an almost liquid material has the properties of a solid. This stage may be observed from the inflection point on a shrinkage-time plot (Fig. 1a), or from the peak on a shrinkage rate-time plot (Fig. 1b). Because the gel point appears at the time  $t_g > t_c$ , the shrinkage stresses appear within the period  $t_g \leq \tau \leq t$ . Then, the shrinkage is limited to the interval  $s_g \leq s \leq s_{\text{max}}$ ,  $Y_g \leq \bar{Y}(E(t)) \leq Y_{\text{max}}$ ,  $\eta_g \leq \bar{\eta}(E(t)) \leq \eta_{\text{max}}$ <sup>2)</sup>.
- In the next considerations, we assume  $t_0 \stackrel{\text{def}}{=} t_g$ .
5. Experimental data show that the Poisson coefficient takes constant value when it passes the gel point [14]. Here, it is assumed to be constant and equal to  $\nu_s$ .

### 2.3. Methodological assumptions

1. The proposed model bases on the linear Maxwell model with time-dependent Young's modulus  $Y(t)$  and the viscosity  $\eta(t)$ <sup>3)</sup>. The total strain rate  $\dot{\epsilon}_{\text{tot}}$  of the system is a sum of a strain rate  $\dot{\epsilon}_s = -\dot{s}$  due to the shrinkage, an elastic strain rate  $\dot{\epsilon}_e$  and a viscous strain rate  $\dot{\epsilon}_v$ :

$$(2.2) \quad \dot{\epsilon}_{\text{tot}} = -\dot{s} + \dot{\epsilon}_e + \dot{\epsilon}_v.$$

The stress rates  $\dot{\sigma}$  in the elastic and viscous elements are the same, and the strain rate  $\dot{\epsilon}$  generating the stress  $\sigma$  is a sum of  $\dot{\epsilon}_e$  and  $\dot{\epsilon}_v$ . If there are no active forces applied to the cured resin, then  $\dot{\epsilon}_{\text{tot}} = 0$ , and  $\dot{\epsilon} = \dot{s}$ .

2. The elastic strain rate and the stress rate are connected by the hypoelastic constitutive equation<sup>4)</sup>, and the viscous strain rate and the stress – by the linear viscous flow rule, namely:

$$(2.3) \quad \dot{\epsilon}_e = \frac{1}{Y(t)} \dot{\sigma}, \quad \text{and} \quad \dot{\epsilon}_v = \frac{1}{\eta(t)} \sigma.$$

3. The constitutive equation connecting the strain rate, shrinkage rate, stress rate and the stress follows from the rules (2.2)–(2.3):

<sup>2)</sup>Usually  $s_g$  exceeds 50%  $s_{\text{max}}$ ,  $Y_g \sim 0.1 \cdot Y_{\text{max}}$  and  $\eta_g \sim 0.03 \cdot \eta_{\text{max}}$  (see [1]).

<sup>3)</sup>The time-dependence includes the exposure function, namely  $Y(t) = \bar{Y}(E(t))$  and  $\eta(t) = \bar{\eta}(E(t))$ .

<sup>4)</sup>Notice that the classical Hooke's law leads to the relation:  $\dot{\epsilon}_e = \frac{1}{Y(t)} \dot{\sigma} - \frac{\dot{Y}(t)}{Y^2(t)} \sigma$ .

$$(2.4) \quad \dot{\varepsilon} = \frac{\dot{\sigma}}{Y(t)} + \frac{\sigma}{\eta(t)} \quad \text{or} \quad \dot{\varepsilon} = \frac{1}{Y(t)} \left( \dot{\sigma} + \frac{\sigma}{\lambda(t)} \right).$$

Here  $\lambda(t) \stackrel{\text{def}}{=} \eta(t)/Y(t)$  is the time-dependent relaxation time.

Because  $Y(t) = \bar{Y}(E(t))$  and  $\eta(t) = \bar{\eta}(E(t))$ , it follows from the rule (2.4) that the total strain  $\varepsilon$  and the total stress  $\sigma$  are functions of two variables: the light exposure  $E(t)$  and time  $t$ , namely: and  $\sigma = \bar{\sigma}(E(t), t)$ . The above fact enables us to separate the curing effects (growth of the Young modulus and the viscosity) from the rheological effects (stress relaxation). Then, for a description of the viscous effects in cured materials, one can introduce a “relaxed” and at the same time – a “growing” Young’s modulus.

Solving the Eq. (2.4) with respect to the stress  $\sigma$ , one can determine the stress changes  $\sigma = \sigma(t)$  accompanying the shrinkage  $s = s(t)$ . To do it, two ways will be applied: a discrete approach and a continuous one. The first approach illustrates the solving procedure; the second one gives an integral rule for the shrinkage stress as a function of time of the light exposure.

### 3. Discrete analysis of the Maxwell model with stepped increasing parameters

At first, let us investigate the Maxwell model with parameters prescribed by the step-wise functions of time. To do it, one can perform the following procedure.

1. As the start point of the shrinkage stress development, is assumed the gel point at the time  $t_0 \stackrel{\text{def}}{=} t_g$  and as the end of the process – the complete setting of the material at the time  $t_n$ . The period  $t_0 \leq t \leq t_n$  includes so-called “dark polymerization phase” which takes place after cutting off the light [22].
2. As the initial Young modulus, is assumed the value  $Y_0 \stackrel{\text{def}}{=} Y_g$ , and as the initial viscosity – the value  $\eta_0 \stackrel{\text{def}}{=} \eta_g$ .
3. The Poisson coefficient is assumed to be constant and equal to the value  $\nu_s$  at the gel point.
4. The time interval  $t_0 \leq \tau \leq t_n$  is divided into  $n$  subintervals:  $t_i \leq \tau \leq t_{i+1}$ , where  $i = 0, \dots, n - 1$  (Fig. 2a).
5. At the time  $t_0$ , the model is composed of a spring with the Young modulus  $Y_0$  and a viscous element with the viscosity  $\eta_0$ .
6. At each next time step  $t_i$  ( $i = 0, \dots, n - 1$ ), we join the original spring with a spring with a constant Young’s modulus  $\Delta Y_i = Y_i - Y_{i-1}$ , and the original viscous element, with a viscous element, with a constant viscosity  $\Delta \eta_i = \eta_i - \eta_{i-1}$ .

7. In effect, we obtain the model which, within each of the time subintervals  $t_i \leq \tau \leq t_{i+1}$ , coincides with the classical Maxwell model.

Notice that the proposed model is different from that known as the generalized Maxwell model. The last one is a bundle of parallel, connected pairs composed of one spring and one viscous element, with fixed properties within the whole interval  $t_0 \leq \tau \leq t_n$  (Fig. 2b). Here, at each of the time steps, the bundle of springs is serially connected with the bundle of viscous elements.

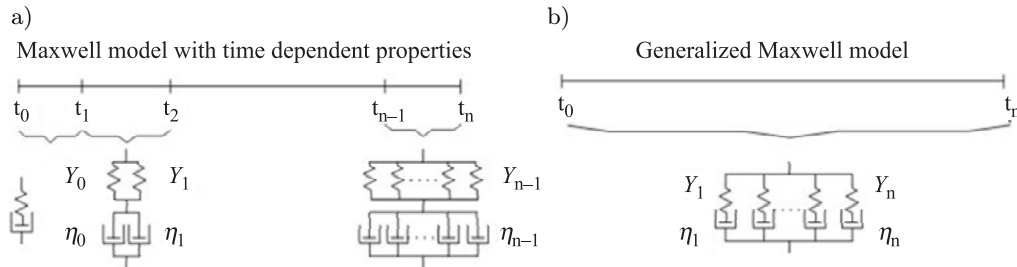


FIG. 2. A comparison of two models: a) the proposed Maxwell model with time-dependent parameters; b) the generalized Maxwell model with fixed parameters.

To find the stress state in the system at each time step  $t_i$ , we proceed as follows.

1. Assume that the system is subjected to a stepped strain function  $\varepsilon = \varepsilon(t)$ . Namely, at the time steps  $t_0, t_1, \dots, t_{n-1}$ , we prescribe constant strains:  $\Delta\varepsilon_0, \Delta\varepsilon_1, \dots, \Delta\varepsilon_{n-1}$  which create immediate elastic reactions through the stresses:  $\Delta\sigma_0^e = Y_0\Delta\varepsilon_0, \Delta\sigma_1^e = Y_1\Delta\varepsilon_1, \dots, \Delta\sigma_{n-1}^e = Y_{n-1}\Delta\varepsilon_{n-1}$ , (Fig. 3a).
2. We assume that each of the stresses  $\Delta\sigma_i^e$  is relaxed in the time interval  $\langle t_i, t_n \rangle$  (Fig. 3b).

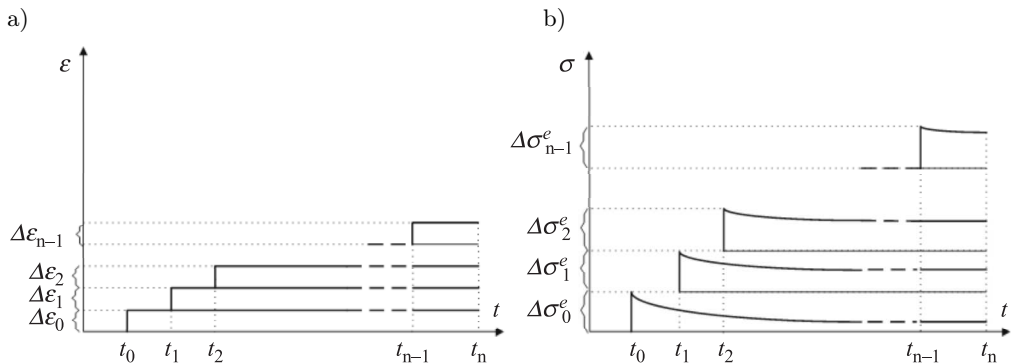
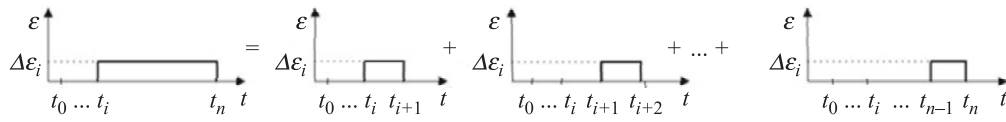
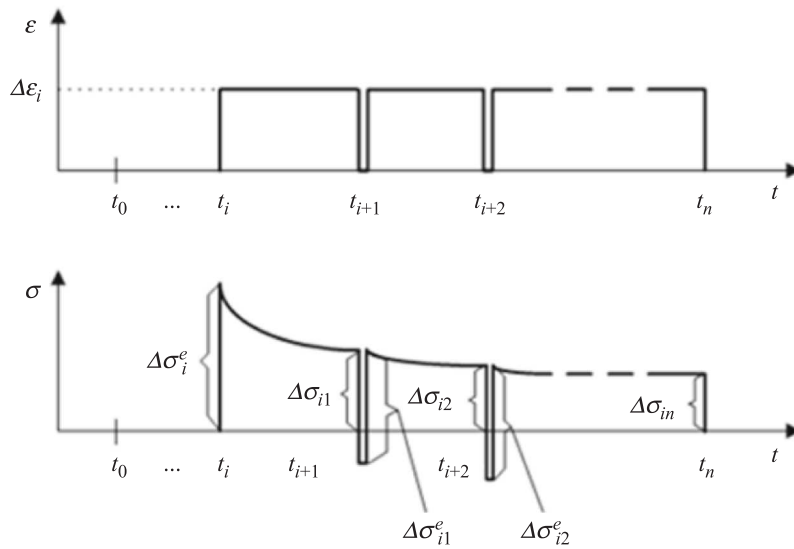


FIG. 3. An assumed behaviour of the model: a) piecewise constant strain increments, b) relaxation of the corresponding elastic stress increments.

FIG. 4. Decomposition of the subinterval  $\langle t_i, t_n \rangle$ .

3. We decompose of the time interval  $\langle t_i, t_n \rangle$  into the sum of subintervals  $\langle t_i, t_{i+1} \rangle, \langle t_{i+1}, t_{i+2} \rangle, \dots, \langle t_{n-1}, t_n \rangle$ , in which the model is described by the fixed parameters  $Y_i, Y_{i+1}, \dots, Y_{n-1}$  and  $\eta_i, \eta_{i+1}, \dots, \eta_{n-1}$  (Fig. 4).
4. The stress  $\Delta\sigma_i^e = Y_i\Delta\varepsilon_i$ , given at the time  $t_i$ , is relaxed to the value  $\Delta\sigma_{i1}^e = Y_i e^{(t_{i+1}-t_i)/\lambda_i}$ , at the time  $t_{i+1}$ . The corresponding relaxation time  $\lambda_i = \eta_i/Y_i$  is constant.
5. To determine the stress  $\Delta\sigma_{i+1}^e$  at the beginning of the next subinterval  $\langle t_{i+1}, t_{i+2} \rangle$ , we put the strain increment  $-\Delta\varepsilon_i$  at the time  $t_{i+1}$ . An additional stress will appear equal to  $-Y_{i+1}\Delta\varepsilon_i$ , which will disappear when we repeat the strain increment  $\Delta\varepsilon_i$  (Fig. 5).

FIG. 5. Relaxation of the stress increment  $\Delta\sigma_j^e$ .

6. Then, the stress  $\Delta\sigma_{i+1}^e$  at the beginning of the subinterval  $\langle t_{i+1}, t_{i+2} \rangle$  is equal to the stress at the end of the previous interval, namely  $\Delta\sigma_{i1}^e = Y_i e^{(t_{i+1}-t_i)/\lambda_i}$ .
7. At the end of the subinterval  $\langle t_{i+1}, t_{i+2} \rangle$ , the stress  $\Delta\sigma_{i1}^e$  is relaxed to the value  $\Delta\sigma_{i2}^e = \Delta\sigma_{i1}^e e^{(t_{i+2}-t_{i+1})/\lambda_i}$ .

8. Then, at the end of the last subinterval  $\langle t_{n-1}, t_n \rangle$ , the following stress appears (Fig. 5):

$$(3.1) \quad \sigma_i \stackrel{\text{def}}{=} \Delta\sigma_{in} = Y_i e^{-\sum_{k=1}^{i-1} \frac{\Delta t_k}{\lambda_k}} \cdot \Delta\varepsilon_i,$$

where  $i = 0, 1, \dots, n-1$ , and  $\Delta t_k \stackrel{\text{def}}{=} t_{k+1} - t_k$ .

9. Finally, at the time  $t_n$ , the total stress  $\sigma_n$  caused by the total strain  $\varepsilon = \sum_{i=0}^{n-1} \Delta\varepsilon_i$  is given by the rule:

$$(3.2) \quad \sigma_n = \sum_{i=0}^{n-1} \Delta\sigma_t = \sum_{i=0}^{n-1} Y_i e^{-\sum_{k=1}^{i-1} \frac{\Delta t_k}{\lambda_k}} \cdot \Delta\varepsilon_i.$$

Notice that the stress increment  $\Delta\sigma_i$ , determined by the following relaxed Young modulus (relaxation function):

$$(3.3) \quad Y_i^{\text{relax}} \stackrel{\text{def}}{=} Y_i \cdot f_i, \quad \text{where} \quad f_i \stackrel{\text{def}}{=} e^{-\sum_{k=1}^{i-1} \frac{\Delta t_k}{\lambda_k}},$$

will be called the ‘‘relaxation factor’’. One can see that to obtain the stress increment  $\Delta\sigma_i$ , for each of the time steps, it is enough to modify the value  $Y_i$  multiplying it by a temporary relaxation factor. However, calculations of stress relaxation require a large number of time steps. The problem disappears when we use a continuous model of the process.

#### 4. 1D visco-hypoelastic model with continuously increasing parameters

The start point is the constitutive Eq. (2.4), given in the form:

$$(4.1) \quad \frac{\dot{\sigma}(t)}{Y(t)} + \frac{\sigma(t)}{\eta(t)} = \dot{\varepsilon}(t).$$

It is valid for each time  $t$  from the interval  $t_0 \leq t \leq t_n$ . To solve the above equation with respect to  $\sigma(t)$ , let us consider the stress change due to a fixed strain increment (step a). Next, basing on the Boltzmann superposition principle, one can pass to the case of the time-dependent strains, through the passage to the limit with the strain increments (step b).

a) *The stress state due to a fixed strain increment*

At a certain time point  $\tau$  from the interval  $t_0 \leq \tau \leq t_n$ , let us prescribe a fixed strain increment  $\Delta\varepsilon_\tau$ . This strain may be expressed by the Heaviside step-function for  $t_0 \leq t \leq t_n$ :

$$(4.2) \quad \Delta\varepsilon_\tau(t) \stackrel{\text{def}}{=} \Delta\varepsilon(t; \tau) = H(t - \tau) \Delta\varepsilon_\tau.$$

If  $\Delta\sigma_\tau(t) \stackrel{\text{def}}{=} \Delta\sigma(t; \tau)$  is the stress increment generated by the strain  $\Delta\varepsilon_\tau$ , then  $\Delta\dot{\varepsilon}_\tau(t) = \delta(t - \tau)\Delta\varepsilon_\tau$ , where  $\delta(t - \tau)$  is the Dirac function. It means that  $\Delta\dot{\varepsilon}_\tau(t) = 0$ , for all time points from the interval  $\tau < t \leq t_n$ . Then, for  $\tau < t \leq t_n$ , the Eq. (4.1) takes the form:

$$(4.3) \quad \frac{\Delta\dot{\sigma}_\tau(t)}{Y(t)} + \frac{\Delta\sigma_\tau(t)}{\eta(t)} = 0 \quad \text{or} \quad \frac{\Delta\dot{\sigma}_\tau(t)}{\Delta\sigma_\tau(t)} = -\frac{1}{\lambda(t)},$$

where  $\lambda(t) = \eta(t)/Y(t)$  is the current relaxation time. One can write the Eq. (4.3) in the form:

$$(4.4) \quad \overline{\ln \Delta\sigma_\tau(t)} = -\frac{1}{\lambda(t)}.$$

Integration of (4.4) leads to the relation:

$$(4.5) \quad \ln \Delta\sigma_\tau(t) = \lim_{t'' \rightarrow \tau} \left\{ \ln \Delta\sigma_\tau(t'') + \int_{t''}^t \left[ -\frac{1}{\lambda(t')} \right] dt' \right\}.$$

However, the time point  $\tau$  is the time of application of the strain increment  $\Delta\varepsilon_\tau(t)$ , when the model is purely hypoelastic, and then

$$(4.6) \quad \lim_{t'' \rightarrow \tau} [\ln \Delta\sigma_\tau(t'')] = \ln[Y(\tau)\Delta\varepsilon_\tau].$$

Finally, one can write the solution of the Eq. (4.3) with respect to  $\Delta\sigma_\tau(t)$ , for  $\tau \leq t \leq t_n$ , in the following form:

$$(4.7) \quad \Delta\sigma_\tau(t) = Y(\tau) \exp\left(-\int_{\tau}^t \frac{dt'}{\lambda(t')}\right) \Delta\varepsilon_\tau.$$

b) *The stress state due to an arbitrary strain*

To describe a stress evolution caused by the photo-curing process, let us look for a function  $\sigma(t)$ , for  $t$  from the interval  $t_0 \leq t \leq t_n$ . To find it, assume that a continuous and differentiable strain  $\varepsilon(\tau)$  is applied in the time  $t_0 \leq \tau \leq t$ . It may be set up through passage to the limit in a superposition of fixed strain increments  $\Delta\varepsilon_\tau$ . In the same way, one can obtain the stress  $\sigma(t)$  generated by the strain  $\varepsilon(\tau)$ , namely

$$(4.8) \quad \begin{aligned} \sigma(t) &= \int_{t_0}^t \Delta\sigma(t; \tau) d\tau = \int_{t_0}^t Y(\tau) \exp\left(-\int_{\tau}^t \frac{dt'}{\lambda(t')}\right) \cdot \frac{\partial\varepsilon(\tau)}{\partial\tau} d\tau \\ &= \int_{t_0}^t Y(\tau) f_\tau(t) \cdot \frac{\partial\varepsilon(\tau)}{\partial\tau} d\tau. \end{aligned}$$

Now, if a relaxation time  $\lambda = \lambda(t)$  is given, one can introduce the relaxed Young's modulus (relaxation function).

$$(4.9) \quad Y_{\tau}^{\text{relax}}(t) \stackrel{\text{def}}{=} Y(\tau) \exp\left(-\int_{\tau}^t \frac{dt'}{\lambda(t')}\right).$$

The relaxation factor (see Eq. (3.3))

$$(4.10) \quad f_{\tau}(t) \stackrel{\text{def}}{=} \exp\left(-\int_{\tau}^t \frac{dt'}{\lambda(t')}\right)$$

indicates an influence of the passage of the time from  $\tau$  to  $t$  on the Young's modulus  $Y(\tau)$  reduction. According to the rule (4.8), to obtain the stress  $\sigma(t)$ , it is enough to multiply the Young's modulus  $Y(\tau)$  by the relaxation factor  $f_{\tau}(t)$  and to integrate the result in the interval  $\langle t_0, t \rangle$ .

### 5. 3D visco-hypoelastic model with time-dependent parameters

The obtained results may be easily adapted to the 3D case. Following Eq. (2.2), the total strain rate tensor  $\dot{\varepsilon}_{ij}^{\text{tot}}$  is a sum of an elastic strain rate tensor  $\dot{\varepsilon}_{ij}^e$ , a viscous strain rate tensor  $\dot{\varepsilon}_{ij}^v$  and the strain rate tensor due to the shrinkage  $\dot{\varepsilon}_{ij}^s = -\dot{s}\delta_{ij}$ . Denote by  $\dot{\varepsilon}_{ij}$  the sum of the elastic and viscous strain rate tensors. Then

$$(5.1) \quad \dot{\varepsilon}_{ij}^{\text{tot}}(t) = \dot{\varepsilon}_{ij}(t) - \dot{s}(t)\delta_{ij}.$$

Denote by  $\varepsilon \stackrel{\text{def}}{=} \varepsilon_{ii}$  the trace of the strain tensor  $\varepsilon_{ij}$ . Then  $\varepsilon_{ij}^* \stackrel{\text{def}}{=} \frac{1}{3}\delta_{ij}\varepsilon$  and  $e_{ij} \stackrel{\text{def}}{=} \varepsilon_{ij} - \frac{1}{3}\delta_{ij}\varepsilon$  will be its volumetric and deviatoric part. Assume that for each time point  $\tau$  from the interval  $t_0 \leq \tau \leq t$ , the Kirchhoff modulus  $G(\tau)$ , the bulk modulus  $K(\tau)$  and the Poisson coefficient  $\nu(\tau)$  of the cured material, are known. Then, a general formulation of 3D constitutive equation yielding from the rule (4.8) takes the form [23]:

$$(5.2) \quad \sigma_{ij}(t) = \int_{t_0}^t 2G(\tau)f_{\tau}^G(t)\dot{e}_{ij}(\tau)d\tau + \delta_{ij} \int_{t_0}^t K(\tau)f_{\tau}^K(t)\dot{\varepsilon}(\tau)d\tau.$$

Here  $f_{\tau}^G(t)$  and  $f_{\tau}^K(t)$  are relaxation factors for  $G(\tau)$  and  $K(\tau)$ . In our model, the Poisson coefficient is assumed to be  $\nu(\tau) = \nu_s = \text{const}$ . One can show that

in this case, the relaxation factors  $f_\tau^G(t)$  and  $f_\tau^K(t)$  must be the same<sup>5)</sup> (see the Appendix):

$$(5.3) \quad f_\tau^G(t) = f_\tau^K(t) = f_\tau(t).$$

Taking into account that  $G(\tau) = Y(\tau)/2(1+\nu_s)$  and  $K(\tau) = Y(\tau)/3(1-2\nu_s)$ , the integral representation of the stress tensor takes the form:

$$(5.4) \quad \sigma_{ij}(t) = \frac{1}{1+\nu_s} \int_{t_0}^t Y(\tau) \left( \dot{\epsilon}_{ij}(\tau) - \frac{1}{3} \cdot \frac{1+\nu_s}{1-2\nu_s} \delta_{ij} \dot{\epsilon}(\tau) \right) f_\tau(t) d\tau$$

or, coming back to the full strain rate tensor  $\dot{\epsilon}_{ij}(\tau)$ , the form:

$$(5.5) \quad \sigma_{ij}(t) = \frac{1}{1+\nu_s} \int_{t_0}^t Y(\tau) \left( \dot{\epsilon}_{ij}(\tau) - \frac{\nu_s}{1-2\nu_s} \delta_{ij} \dot{\epsilon}(\tau) \right) f_\tau(t) d\tau.$$

Concluding, to obtain the stress  $\sigma_{ij}(t)$ , it is enough to find the relaxed Young's modulus  $Y_\tau^{\text{relax}}(t) = Y(\tau) \cdot f_\tau(t)$ , and next to use the standard procedure for the hypoelastic materials [24]. It is necessary to point out that the number of assumed time steps has no influence on the accuracy of the viscous effects modelling, because the relaxation factor  $f_\tau(t)$  is given explicitly by Eq. (4.10). However, higher number of the time steps may improve the input of material data.

## 6. Shrinkage stress evolution for the composite Clearfil F2

### 6.1. Material data

To determine shrinkage stresses in a photo-cured specimen, it is necessary to know the values of material parameters on each step of the process. Then, it is necessary to determine the Young's modulus  $Y(t)$ , the relaxation time  $\lambda(t)$  and the strain  $\varepsilon(t) = s(t)$  for  $t_0 \leq t \leq t_n$ . One can use the data for the chemically activated Clearfil F2 [1] cured after 3580 s. The same Clearfil F2 may be photo-cured after 40 seconds, if we use a photo-initiator. Adjustment of data given in the paper [1] leads to the values of shrinkage  $s$ , Young's modulus  $Y$ , viscosity  $\eta$  and relaxation time  $\lambda$ , given in Table 1. The Poisson coefficient is fixed and taken as  $\nu_s = 0.24$ .

The adjustment of the material data is made as follows. The data for  $s$ ,  $Y$ ,  $\eta$ , and  $\lambda$  given in the paper [1] have been referred to the time steps  $t_1^{ch}, t_2^{ch}, \dots, t_8^{ch}$ .

<sup>5)</sup>The rule (5.2) and the assumption (5.3) are taken in the procedure based on the Maxwell model with fixed parameters in the Abaqus system [24].

In Table 1, the same values are referred to the time steps  $t_i = t_i^{ch} \cdot (40/3580)$ . It means that the time scale has been reduced proportionally. One can do it, if the material parameters do not depend on the polymerization rate. In our case, these parameters are functions of the polymer conversion degree only (cf. Sec. 2.1 and 2.2).

**Table 1. Input data (according to [1]).**

| Step  | Time [s] | $s$ [%] | $Y$ [MPa] | $\eta$ [MPa s] | $\lambda$ [s] |
|-------|----------|---------|-----------|----------------|---------------|
| $t_1$ | 3.13     | 0.200   | 100       | 0              | 0.00          |
| $t_2$ | 4.25     | 0.500   | 1100      | 2800           | 2.54          |
| $t_3$ | 6.48     | 0.600   | 3700      | 26800          | 7.24          |
| $t_4$ | 9.83     | 0.700   | 5700      | 109100         | 19.14         |
| $t_5$ | 17.37    | 0.725   | 6725      | 288050         | 42.83         |
| $t_6$ | 24.91    | 0.750   | 7750      | 467000         | 60.25         |
| $t_7$ | 32.46    | 0.775   | 8775      | 645950         | 73.61         |
| $t_8$ | 40.00    | 0.800   | 9800      | 824900         | 84.17         |

The shrinkage-time plot (Fig. 1) and the Young modulus-time plot (Fig. 6) point out the time  $t_g = 4.25$  s as the gel point. It is assumed as the start point  $t_2 = 4.25$  s for the analysis. The end of the photo-curing process is taken as

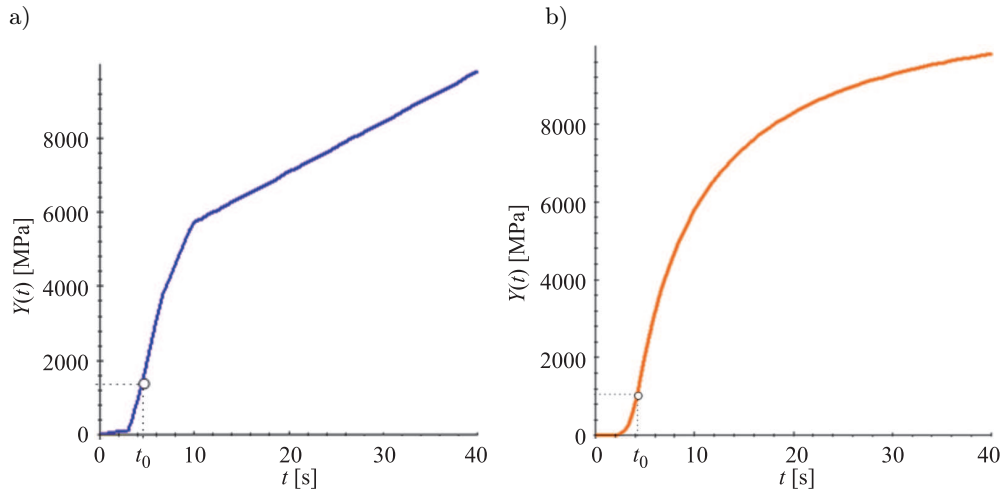


FIG. 6. The Young modulus for Clearfil F2: a) the piecewise linear plot connecting the experimental data [1], b) its smooth approximation (Eq.(6.2)).

$t_8 = 40$  s. On the basis of the data given in Table 1, one can plot the piecewise linear functions  $\dot{s}(t)$  and  $\lambda^{-1}(t)$  (Fig. 7).

## 6.2. A smooth approximation of the material data functions

To use the Eq. (4.8) effectively, one can introduce smooth approximations of the piecewise linear functions  $\dot{s}(t)$ ,  $Y(t)$  and  $\lambda^{-1}(t)$  for the time  $t_0 \leq t \leq t_n$ . Because the period  $t_0 \leq t \leq t_n$  succeeds the glass point, a rapid change of the process character (Fig. 1a) cannot appear. The auto-acceleration effect connected with the glass point is outside of the considered period [25]. Then, one can assume smooth approximations of the reflected functions in the following way<sup>6)</sup>.

Denote by  $A(t)$  one of these functions. As an approximation of  $A(t)$ , one can assume a smooth function:

$$(6.1) \quad A_{\text{approx}}(t) = \frac{a}{t+b} + c.$$

Here, three constants  $a$ ,  $b$ ,  $c$  are determined from three conditions:  $A(t_2) = A_{\text{approx}}(t_2)$ ,  $A(t_4) = A_{\text{approx}}(t_4)$  and  $A(t_8) = A_{\text{approx}}(t_8)$ <sup>7)</sup>. In this way we obtain three smooth functions:

$$(6.2) \quad \dot{s}(\tau) = \frac{a_s}{\tau + b_s} + c_s, \quad Y(\tau) = \frac{a_m}{\tau + b_m} + c_m, \quad \lambda^{-1}(\tau) = \frac{a_\lambda}{\tau + b_\lambda} + c_\lambda.$$

where constants  $a_s$ ,  $b_s$ ,  $c_s$ ,  $a_m$ ,  $b_m$ ,  $c_m$ ,  $a_\lambda$ ,  $b_\lambda$ ,  $c_\lambda$ , are given in Table 2.

**Table 2. Fitting parameters for smooth approximations of the material data functions.**

| Coefficient | $\dot{s}(t)$                   | $Y(t)$           | $\lambda^{-1}(t)$                   |
|-------------|--------------------------------|------------------|-------------------------------------|
| $a$         | $a_s = 2.0337 \times 10^{-3}$  | $a_m = -7364900$ | $a_\lambda = 0.31239$               |
| $b$         | $b_s = -3.4946$                | $b_m = 2.8223$   | $b_\lambda = -3.4455$               |
| $c$         | $c_s = -2.2562 \times 10^{-5}$ | $c_m = 11520$    | $c_\lambda = 3.3348 \times 10^{-3}$ |

Figure 7 shows a comparison of the piecewise linear functions  $\dot{s}(t)$ ,  $Y(t)$ ,  $\lambda^{-1}(t)$ , with their smooth approximations.

A higher number of fitting parameters in Eq. (6.1) gives better approximations, but this change has small influence on the results.

<sup>6)</sup>The way of approximation is the one possible; it is adapted to the shape of the given piecewise-linear functions.

<sup>7)</sup>The time-points  $t_2$ ,  $t_4$ ,  $t_8$  correspond to the beginning, the gel-point, and the end of these process.

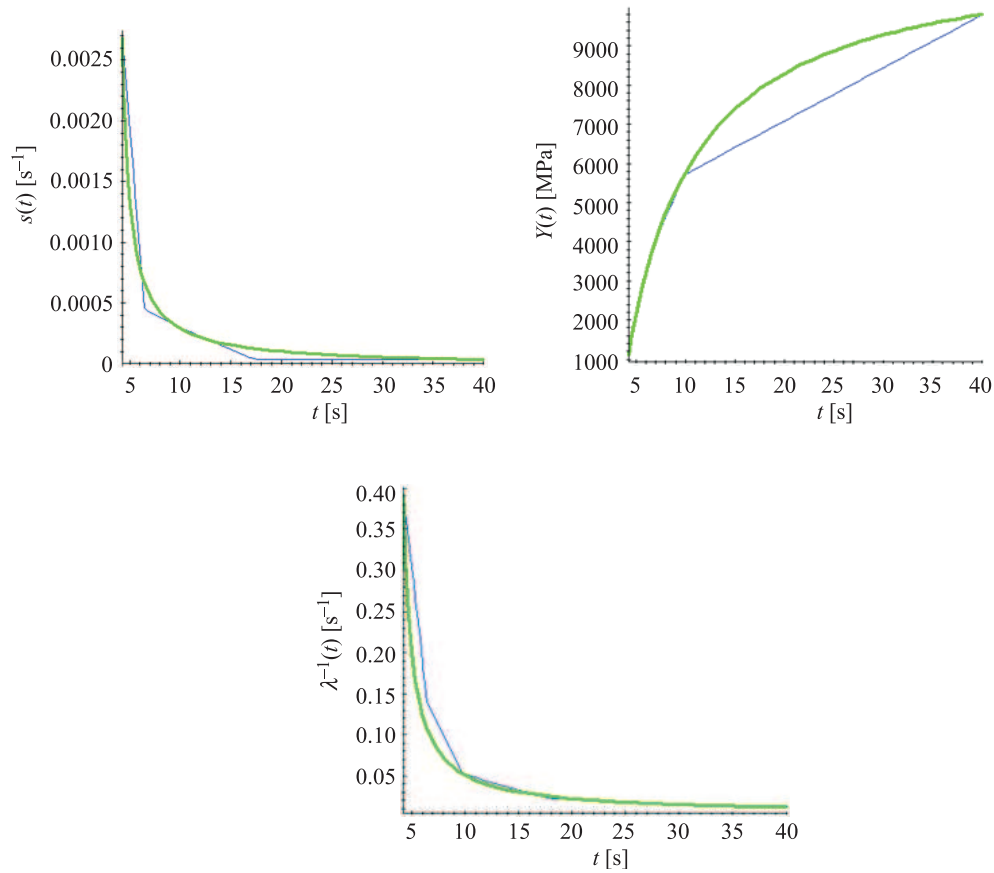


FIG. 7. The piecewise linear functions  $\dot{s}(t)$ ,  $Y(t)$  and  $\lambda^{-1}(t)$ , and their smooth approximations for Clearfil F2.

### 6.3. The relaxation factor

If we introduce the function  $\lambda^{-1}(t')$  given by Eq. (6.2) into Eq. (4.10), the relaxation factor  $f_\tau(t)$  will take the following form:

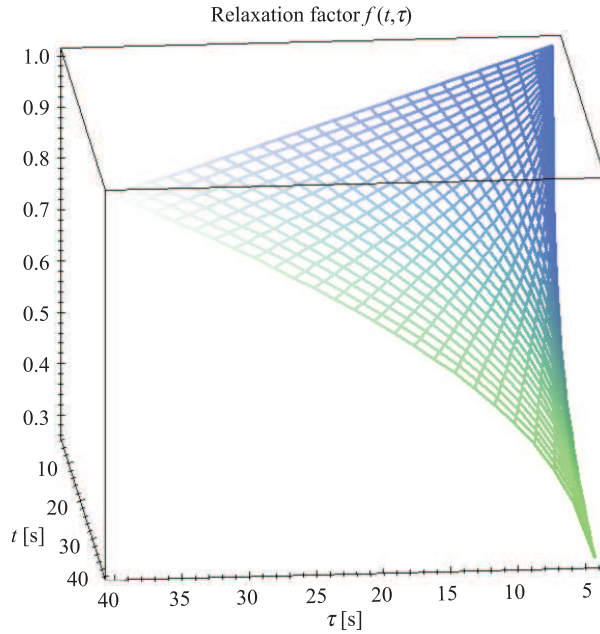
$$(6.3) \quad f_\tau(t) = \left( \frac{\tau + b_\lambda}{t + b_\lambda} \right)^{a_\lambda} \cdot e^{-c_\lambda(t-\tau)},$$

where  $a_\lambda$ ,  $b_\lambda$  and  $c_\lambda$  are given in Table 2. The values of  $f_\tau(t)$  at the time points  $\tau = t_2, \dots, t_8$  and  $t = t_2, \dots, t_8$  are given in Table 3. The last column gives the values of the relaxation factor  $f_{\tau_i}(t_8)$  for the case of cured material. According to the rule (4.8), the final shrinkage stress  $\sigma(t_8)$  is determined by the values  $f_{\tau_i}(t_8)$  and  $Y(\tau_i)$  for  $i = 2, \dots, 8$ .

The 2D plot of the relaxation factor  $f_\tau(t)$  (see Eq. (6.3)) is shown in Fig. 8.

**Table 3.** Values of the relaxation factor  $f_{\tau=\tau_i}(t = t_i)$  for  $i = 1, 2, \dots, 8$ .

|          | $t_2$ | $t_3$  | $t_4$  | $t_5$  | $t_6$  | $t_7$  | $t_8$         |
|----------|-------|--------|--------|--------|--------|--------|---------------|
| $\tau_2$ | 1.000 | 0.6545 | 0.5130 | 0.3921 | 0.3340 | 0.2965 | <b>0.2690</b> |
| $\tau_3$ | –     | 1.000  | 0.7838 | 0.5991 | 0.5103 | 0.4530 | <b>0.4110</b> |
| $\tau_4$ | –     | –      | 1.000  | 0.7644 | 0.6511 | 0.5780 | <b>0.5244</b> |
| $\tau_5$ | –     | –      | –      | 1.000  | 0.8519 | 0.7561 | <b>0.6860</b> |
| $\tau_6$ | –     | –      | –      | –      | 1.0000 | 0.8876 | <b>0.8053</b> |
| $\tau_7$ | –     | –      | –      | –      | –      | 1.0000 | <b>0.9073</b> |
| $\tau_8$ | –     | –      | –      | –      | –      | –      | <b>1.0000</b> |

FIG. 8. The relaxation factor  $f_{\tau}(t) \stackrel{\text{def}}{=} \exp(-\int_{\tau}^t \frac{dt'}{\lambda(t')})$  for Clearfil F2.

The product of the smooth functions described by Eq. (6.2) and Eq. (6.3) gives the relaxed Young modulus:

$$(6.4) \quad Y_{\tau}^{\text{relax}}(t) = \left( \frac{a_m}{\tau + b_m} + c_m \right) \left( \frac{\tau + b_{\lambda}}{t + b_{\lambda}} \right)^{a_{\lambda}} \cdot e^{-c_{\lambda}(t-\tau)},$$

where  $a_m$ ,  $b_m$  and  $c_m$  are given in Table 2. The plots of  $Y_{\tau}^{\text{relax}}(t)$  for  $\tau = t_2, \dots, t_8$  are shown in Fig. 9.

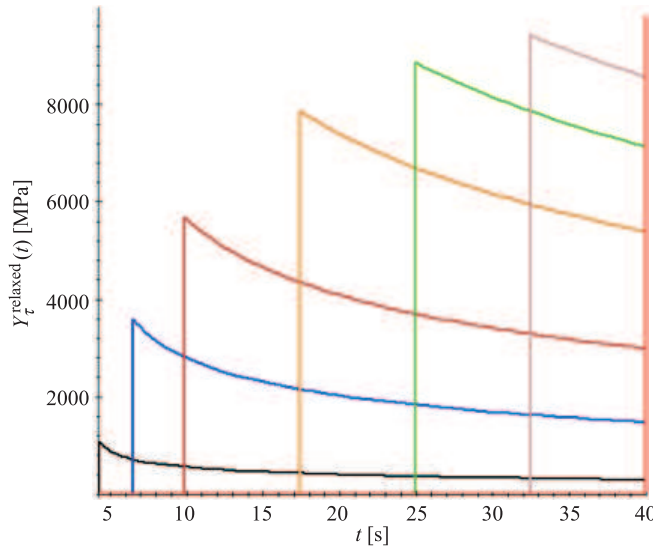


FIG. 9. The relaxed Young modulus  $Y_{\tau}^{\text{relax}}(t) = Y(t) \cdot f_{\tau}(t)$ , for  $\tau = t_2, \dots, t_8$ .

#### 6.4. The shrinkage stress

According to the rule (4.8), the basic influence on the shrinkage stress level has the strain rate determined by the shrinkage rate. The smooth strain rate function  $\dot{\varepsilon}(\tau)$  has the form:

$$(6.5) \quad \dot{\varepsilon}(\tau) = \dot{s}(\tau) = \frac{a_s}{\tau + b_s} + c_s,$$

where  $a_s$ ,  $b_s$  and  $c_s$  are given in Table 2. The expression for the shrinkage stress follows from Eq. (4.8) and the relations (6.4)–(6.5).

$$(6.6) \quad \sigma(t) = \int_{t_0}^t \left( \frac{a_m}{\tau + b_m} + c_m \right) \left( \frac{a_s}{\tau + b_s} + c_s \right) \left( \frac{\tau + b_{\lambda}}{t + b_{\lambda}} \right)^{a_{\lambda}} \cdot e^{-c_{\lambda}(t-\tau)} d\tau.$$

REMARK. The stress  $\sigma(t)$  is determined uniquely by the set of nine constants:  $a_m$ ,  $b_m$ ,  $c_m$ ,  $a_s$ ,  $b_s$ ,  $c_s$ ,  $a_{\lambda}$ ,  $b_{\lambda}$ ,  $c_{\lambda}$ , calculated on the basis of given material data.

To integrate the expression (6.6), one can write it in the form:

$$(6.7) \quad \sigma(t) = g(t) \cdot \int_{t_0}^t h(\tau) d\tau,$$

where

$$(6.8) \quad g(t) \stackrel{\text{def}}{=} \left( \frac{1}{t + b_{\lambda}} \right)^{a_{\lambda}} e^{-c_{\lambda}t},$$

and

$$(6.9) \quad h(\tau) \stackrel{\text{def}}{=} \left( \frac{a_m}{\tau + b_m} + c_m \right) \left( \frac{a_s}{\tau + b_s} + c_s \right) (\tau + b_\lambda)^{a_\lambda} \cdot e^{c_\lambda \tau}.$$

Because  $h(\tau)$  is a product of a rational function and an exponential function, its integral may be a non-elementary one. Integration of the function  $h(\tau)$  using standard numerical procedures causes some difficulties. To avoid the problem, we assume the following approximation of the function  $h(\tau)$ :

$$(6.10) \quad h_{\text{approx}}(\tau) = \frac{\tau}{a_h \tau^2 + b_h \tau + c_h},$$

where the constants  $a_h, b_h, c_h$  are determined from the conditions merging both functions at the time-points:  $t_2, t_4$  and  $t_8$ . We obtain:  $a_h = 0.021462$ ,  $b_h = -0.012938$  and  $c_h = 1.1877$ . A comparison of the plots  $h(\tau)$  and  $h_{\text{approx}}(\tau)$  is shown in Fig. 10.

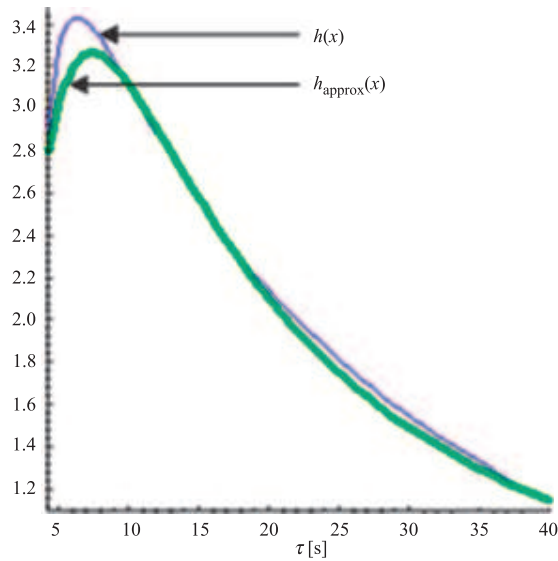


FIG. 10. The plots of the functions  $h(\tau)$  and  $h_{\text{approx}}(\tau)$ .

Then, if the material data  $s(t)$ ,  $Y(t)$  and  $\eta(t)$  are given, one can get the shrinkage stress from the rules (6.7)–(6.10). The results for the composite Clearfil F2 are presented in Fig. 11. Values of the stress at the assumed time-points are given in Table 4. The final stress, in the cured material, is equal to 21.26 MPa.

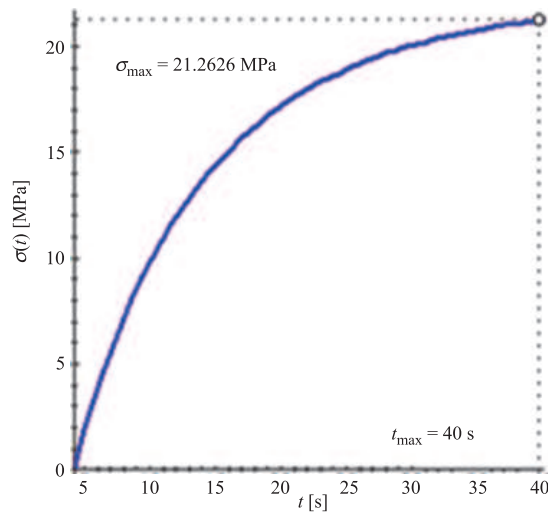


FIG. 11. Time-evolution of the visco-hypoelastic stress in the photo-cured composite Clearfil F2.

Table 4. Values of the shrinkage stress in Clearfil F2 for time steps  $t_2, \dots, t_8$ .

| Step  | Time [s]     | $\sigma$ [MPa] |
|-------|--------------|----------------|
| $t_2$ | 4.25         | 0.00           |
| $t_3$ | 6.48         | 4.74           |
| $t_4$ | 9.83         | 9.58           |
| $t_5$ | 17.37        | 15.87          |
| $t_6$ | 24.92        | 18.90          |
| $t_7$ | 32.46        | 20.46          |
| $t_8$ | <b>40.00</b> | <b>21.26</b>   |

## 7. Concluding remarks

### 7.1. Comparison with other models

Denote by  $\sigma_{\text{visco-hypo}}(t)$  the function describing a shrinkage stress evolution given by Eq. (4.8), which follows from the proposed model. Remember that  $\sigma_{\text{visco-hypo}}(t_8) = 21.2626$  MPa. Let us compare values of the highest shrinkage stresses obtained by means of some simplifications of the rule (4.8).

The photo-curing process may be considered as an elastic one with a variable Young's modulus [26]. If we put  $f_\tau(t) \equiv 1$  in Eq. (4.8), we obtain an integral form of the hypoelastic constitutive relation

$$(7.1) \quad \sigma_{\text{hypo}}(t) = \int_{t_0}^t Y(\tau) \frac{\partial \varepsilon(\tau)}{\partial \tau} d\tau = \int_{t_0}^t \left( \frac{a_m}{\tau + b_m} + c_m \right) \left( \frac{a_s}{\tau + b_s} + c_s \right) d\tau.$$

From the above rule, it follows that the highest shrinkage stress is equal to  $\sigma_{\text{hypo}}(t_8) = 35.5853$  MPa. Then, the hypoelastic model gives the highest stresses near 70% larger than the proposed model with a relaxed Young's modulus.

To take into account the stress relaxation, one can assume a fixed, averaged relaxation factor  $f_a$  in Eq. (4.8), namely

$$(7.2) \quad f_a \stackrel{\text{def}}{=} e^{-\frac{t_n - t_0}{\lambda_a}},$$

where

$$(7.3) \quad \lambda_a \stackrel{\text{def}}{=} \frac{1}{n} \sum_{i=0}^{n-1} \lambda_i.$$

Then, the corresponding stress will take the form

$$(7.4) \quad \sigma_{\text{mod-hypo}}(t) = f_a \cdot \int_{t_0}^t Y(\tau) \frac{\partial \varepsilon(\tau)}{\partial \tau} d\tau,$$

with the highest shrinkage stress equal to the value  $\sigma_{\text{mod-hypo}}(t_8) = 15.0029$  MPa. This model gives the highest stresses near 30% lower than the proposed one. A comparison of the plots for  $\sigma_{\text{visco-hypo}}$ ,  $\sigma_{\text{hypo}}(t)$  and  $\sigma_{\text{mod-hypo}}(t)$  is given in Fig. 12.

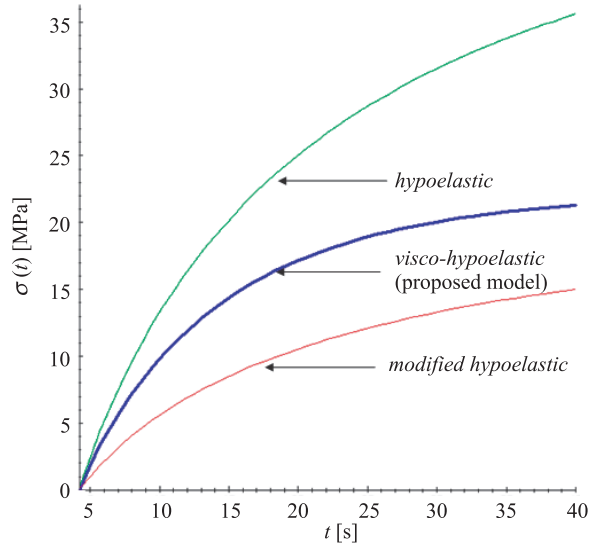


FIG. 12. A comparison of shrinkage stresses obtained with the help of three models.

## 7.2. Comparison with experimental data

Most of experiments show that shrinkage stresses in 3D cured layers of dental composites, placed between two discs, do not exceed 10 MPa [27]. On the other hand, the value  $\sigma_{\text{visco-hypo}}(t_8) = 21.26$  MPa was obtained under the assumption of 1D stress-strain state in the cured composite. In the 3D cured layer, a non-uniform displacement field appears. A measure of this non-uniformity is the C-factor determined as the ratio of adhered to the free surface of the cured composite layer [28]. Then, to confirm our result experimentally, it is necessary to use in tests a very thin layer.

The influence of layer thickness on the curing stress in thin resin layers for the composite Clearfill F2 was investigated in the paper [18]. A chemically initiated resin composite layer was inserted between two discs in a tensiometer. Next, the curing contraction of the composite layers was corrected by feedback displacement of the tensiometer, and the curing stress development was registered<sup>8)</sup>. The shrinkage stress was determined for layer thicknesses from 50  $\mu\text{m}$  to 2.7 mm. After 20 min of the process, the Young's modulus was equal to 9300 MPa<sup>9)</sup>. Conclusion of the Authors was the following: "the contraction stress after 20 min decreased from  $23.3 \pm 5.3$  MPa for the 50 microns layer to  $5.5 \pm 0.6$  MPa for the 2.7 mm layer".

Notice that the highest value of the Young's modulus assumed in our calculations has been reached after 3580 s of the chemical curing [1], or after 40 s of the photo curing. Here in [18], the chemical process ran three times faster, and the similar value of the Young's modulus has been reached after 1200 s. It means that in the photo-curing process, the time scale must be reduced proportionally with the coefficient 40/1200.

Figure 13 presents a comparison of the function  $\sigma_{\text{visco-hypo}}(t)$  (Fig. 12) with the measured mean-cured stresses, for various layer thicknesses. Notice that this function with the highest value 21.26 MPa, corresponds to the layer thickness close to the value 100  $\mu\text{m}$ . A question appears: how thin layers may give a correct prediction of the shrinkage stresses? It seems that for layers thinner than 100  $\mu\text{m}$ , the compliance of the experimental set-up and some microscopic effects may have an essential influence on the results.

One can state that the proposed visco-hypoelastic model gives good results for the photo-curing processes with a long exposure time. Then the temperature has no real influence on the process. The above assumption is not valid in the case

---

<sup>8)</sup>Because compliance of the system was fixed and equal to 0.029 mm/MPa, the measurement accuracy for the very thin layers was much lower than that for the thicker layers.

<sup>9)</sup>Recall that the highest value of the Young's modulus assumed in our calculations is equal to 9800 MPa.

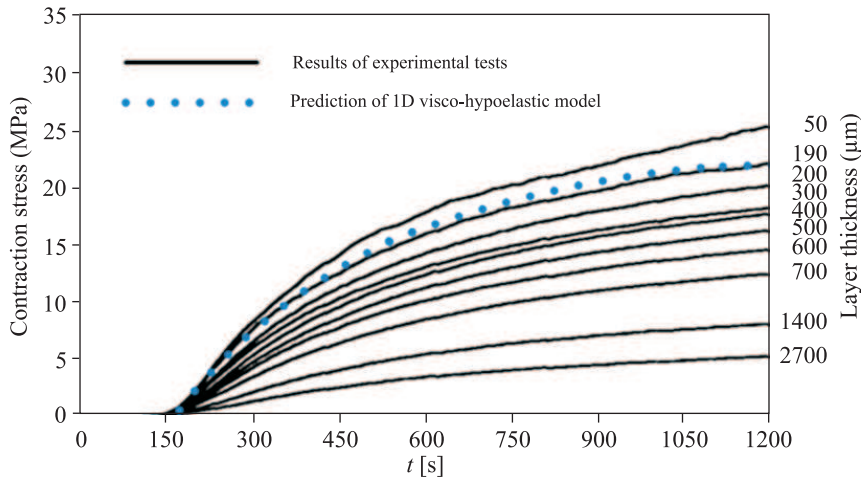


FIG. 13. A comparison of shrinkage stresses prescribed by Eq. (4.8) with experimental results (according to [21]).

of the process of the stereolithography. In this case, one can apply the concepts of the temperature-reduced time scale [29–30].

### Appendix: Remarks on 3D shrinkage stresses

Let us consider a unidirectional shrinkage in a 3D bar made of the composite Clearfil F2. In an orthogonal system of coordinates, a uniform strain field is given by the tensor

$$(A.1) \quad \dot{\varepsilon}_{ij} = \dot{s}(t) \begin{bmatrix} 1 & 0 & 0 \\ 0 & -\nu_s & 0 \\ 0 & 0 & -\nu_s \end{bmatrix}.$$

The volumetric and the deviatoric part of the tensor take the form:

$$(A.2) \quad \begin{aligned} \varepsilon_{ij}^*(t) &= \varepsilon(t) \sigma_{ij} = \dot{s}(t)(1 - 2\nu_s) \delta_{ij} \\ \dot{\varepsilon}_{ij}(t) &= \dot{s}(t) \frac{2}{3}(1 + \nu_s) \begin{bmatrix} 1 & 0 & 0 \\ 0 & -\frac{1}{2} & 0 \\ 0 & 0 & -\frac{1}{2} \end{bmatrix}. \end{aligned}$$

To find the stress tensor  $\sigma_{ij}$ , let us use for a moment the general rule (5.2) with the independent relaxation factors  $f_\tau^G(t)$  and  $f_\tau^K(t)$ . Substituting

$G(\tau) = Y(\tau)/2(1 + \nu_s)$  and  $K(\tau) = Y(\tau)/3(1 - 2\nu_s)$  into Eq. (5.2), we get:

$$(A.3) \quad \sigma_{11} = \frac{1}{3} \int_{t_0}^t Y(\tau)[2f_{\tau}^G(t) + f_{\tau}^K(t)]\dot{s}(\tau)d\tau,$$

$$(A.4) \quad \sigma_{22}(t) = \sigma_{33}(t) = \frac{1}{3} \int_{t_0}^t Y(\tau)[-f_{\tau}^G(t) + f_{\tau}^K(t)](\tau)d\tau,$$

$$(A.5) \quad \sigma_{12}(t) = \sigma_{13}(t) = \sigma_{23}(t) = 0.$$

One can see that the conditions

$$(A.6) \quad \sigma_{22}(t) = \sigma_{33}(t) = 0$$

are satisfied when  $f_{\tau}^G(t) = f_{\tau}^K(t) = f_{\tau}(t)$ . Moreover, in this case  $\sigma_{11}(t)$  in the considered 3D bar is the same as the stress  $\sigma(t)$  obtained for the 1D model.

## References

1. B.S. DAUVILLIER, A.J. FEILZER, A.J. DE GEE, C.L. DAVIDSON, *Visco-elastic parameters of dental restorative materials during setting*, J. Dental Research, **79**, 818–823, 2000.
2. A.J. FEILZER, B.S. DAUVILLIER, *Effect of TEGMA/BisGMA ratio on stress development and viscoelastic properties of experimental two-paste composites*, J. Dental Research, **82**, 824–828, 2003.
3. R. AJLOUNI, S.E. BISHARA, M.M. SOLIMAN, C. OONSOMBAT, J.F. LAFFOON, J. WARREN, *The use ofOrmocer as an alternative material for bonding orthodontic brackets*, Angle Orthod., **75**, 106–108, 2005.
4. A. VERSLUIS, W.H. DOUGLAS, M. CROSS, *Does an incremental filling technique reduce polymerization shrinkage stress?* J. Dental Research, **75**, 871–878, 1996.
5. A. VERSLUIS, D. TANTBIROJN, W.H. DOUGLAS, *Does dental composites always shrink toward the light?* J. Dental Research, **77**, 1435–1445, 1998.
6. P. KOWALCZYK, W. GAMBIN, *Techniques of shrinkage stress reduction in dental restoration*, International Journal of Material Forming, **1**, 755–758, 2008.
7. P. KOWALCZYK, *Influence of the shape of the layers in photo-cured dental restorations on the shrinkage stress peaks – FEM study*, Dental Materials, **25**, e83–e91, 2009.
8. B.S. DAUVILLIER, P.F. HÜBSH, M.P. AARNTS, A.J. FEILZER, *Modeling of viscoelastic behavior of dental chemically activated composites during curing*, Journal of Biomedical Materials Research Part B: Applied Biomaterials, **58**, 16–26, 2001.
9. M.M. WINKLER, T.R. KATONA, N.H. PAYDAR, *Finite element stress analysis of three filling techniques for class V light-cured composites restorations*, J. Dental Research, **75**, 1477–1483, 1996.

10. *Abaqus Analysis User's Manual*, Vol. 6.7, Section 17.4.1, *Hypoelastic behavior*, Hibbitt, Karlsson and Sorensen Inc., 2008.
11. C. TRUESDELL, *Hypoelasticity*, *J. Ration. Mech. Anal.* **4**, 83–133, 1955.
12. A.C. ERINGEN, *Nonlinear Theory of Continuous Media*, McGraw-Hill, 1962.
13. P.F. HÜBSH, J. MIDDLETON, J. KNOX, *A finite element analysis of the stress at the restoration-tooth interface, comparing inlays and bulk fillings*, *Biomaterials*, **21**, 1015–1019, 2000.
14. M. BARINK, P.C.P VAN DER MARK, W.M.M. FENNIS, R.H. KUIJS, C.M. KREULEN, N. VERDONSCHOT, *A three-dimensional finite element model of the polymerization process in dental composites*, *Biomaterials*, **24**, 1427–1435, 2003.
15. D.L. HUSSEY, P.A. BIAGIONI, P.J. LAMEY, *Thermographic measurement of temperature change during resin composite polymerization in vivo*, *Journal of Dentistry*, **23**, 267–271, 1995.
16. F.P. JACOBS, *Rapid prototyping & manufacturing, fundamentals of stereolithography*, Society of manufacturing engineers, Dearborn, MI, USA 1992.
17. F. RUEGGERBERG, K. TAMARESELY, *Resin cure determination by polymerization shrinkage*, *Dental Materials*, **11**, 265–268, 1995.
18. D. ALSTER, A.J. FEILZER, A.J. DE GEE, C.L DAVIDSON, *Polymerization contraction stress in thin resin composite layers as a function of layer thickness*, *Dental Materials*, **13**, 146–150, 1997.
19. Y.M. HUANG, C.P. JIANG, *Curl distortion analysis during photo polymerization of stereolithography using dynamic finite element method*, *Int. J. Adv. Manuf. Technol.*, **21**, 586–595, 2003.
20. Y.M. HUANG, C.P. JIANG, *Numerical analysis of a mask type stereolithography process using a dynamic finite-element method*, *Int. J. Adv. Manuf. Technol.*, **21**, 649–655, 2003.
21. Y.M. HUANG, J.Y. JENG, C.P. JIANG, *Increased accuracy by using dynamic finite element method in the constrain-surface stereolithography system*, *J. Mat. Proc. Tech.*, **140**, 191–196, 2003.
22. E. ANDRZEJEWSKA, *Photopolymerization kinetics of multifunctional monomers*, *Prog. Polym. Sci.*, **26**, 605–665, 2001.
23. A.C. PIPKIN, T.G. ROGERS, *A nonlinear integral representation for viscoelastic behavior*, *J. Mech. Phys. Solids*, **16**, 59–72, 1968.
24. *Abaqus Theory Manual*, Vol. 6.7, Section 4.1.8, *Viscoelasticity*, Hibbitt, Karlsson and Sorensen Inc., 2008.
25. G. ELIADES, D.C.WATTS, T. ELIADES [Eds.], *Dental Hard Tissues and Bonding*, Springer, Berlin, Heidelberg 2005.
26. A. VEARSULIS, D. TANTBIROJN, M.R. PINTADO, R. DE LONG, W.H. DOUGLAS, *Residual shrinkage stress distributions in molars after composite restoration*, *Dental Materials*, **20**, 554–564, 2004.
27. R.R. BRAGA, J.L. FERRACANE, *Contraction stress related to degree of conversion and reaction kinetics*, *J. Dental Research*, **81**, 114–118, 2002.

28. A.J. FEILZER, A.J. DE GEE, C.L. DAVIDSON, *Setting stress in composite resin in relation to configuration of the restoration*, J. Dental Research, **66**, 1636–1639, 1987.
29. L.W. MORLAND, E.H. LEE, *Stress analysis for linear viscoelastic materials with temperature variation*, Transaction of the Society of Rheology, **4**, 233–263, 1960.
30. M.L. WILLIAMS, R.F. LANDEL, J.D. FERRY, *Structural analysis of viscoelastic materials*, AIAA Journal, **5**, 785–808, 1964.

*Received February 28, 2010; revised version August 13, 2010.*

---